

# Autophosphorylation of *Archaeoglobus fulgidus* Rio2 and crystal structures of its nucleotide–metal ion complexes

Nicole LaRonde-LeBlanc<sup>1</sup>, Tad Guszczynski<sup>2</sup>, Terry Copeland<sup>2</sup> and Alexander Wlodawer<sup>1</sup>

<sup>1</sup> Protein Structure Section, Macromolecular Crystallography Laboratory, National Cancer Institute, NCI-Frederick, MD USA

<sup>2</sup> Laboratory of Protein Dynamics and Signaling, National Cancer Institute, NCI-Frederick, MD USA

## Keywords

autophosphorylation; nucleotide complex; protein kinase; ribosome biogenesis; Rio2

## Correspondence

A. Wlodawer, National Cancer Institute,  
MCL Bldg. 536, Rm. 5, Frederick,  
MD 21702–1201, USA  
Fax: +1 301 846 6322  
Tel: +1 301 846 5036  
E-mail: wlodawer@ncifcrf.gov

(Received 9 February 2005, revised 1 April 2005, accepted 5 April 2005)

doi:10.1111/j.1742-4658.2005.04702.x

The highly conserved, atypical RIO serine protein kinases are found in all organisms, from archaea to man. In yeast, the kinase activity of Rio2 is necessary for the final processing step of maturing the 18S ribosomal rRNA. We have previously shown that the Rio2 protein from *Archaeoglobus fulgidus* contains both a small kinase domain and an N-terminal winged helix domain. Previously solved structures using crystals soaked in nucleotides and Mg<sup>2+</sup> or Mn<sup>2+</sup> showed bound nucleotide but no ordered metal ions, leading us to the conclusion that they did not represent an active conformation of the enzyme. To determine the functional form of Rio2, we crystallized it after incubation with ATP or ADP and Mn<sup>2+</sup>. Co-crystal structures of Rio2–ATP–Mn and Rio2–ADP–Mn were solved at 1.84 and 1.75 Å resolution, respectively. The  $\gamma$ -phosphate of ATP is firmly positioned in a manner clearly distinct from its location in canonical serine kinases. Comparison of the Rio2–ATP–Mn complex with the Rio2 structure with no added nucleotides and with the ADP complex indicates that a flexible portion of the Rio2 molecule becomes ordered through direct interaction between His126 and the  $\gamma$ -phosphate oxygen of ATP. Phosphopeptide mapping of the autophosphorylation site of Rio2 identified Ser128, within the flexible loop and directly adjacent to the part that becomes ordered in response to ATP, as the target. These results give us further information about the nature of the active site of Rio2 kinase and suggest a mechanism of regulation of its enzymatic activity.

Protein kinases play an important role in the regulation of most cellular processes. As such, they are recognized as a major group of targets for therapeutic drug development. Over 500 protein kinases that have been identified in human cells [1] can be divided into two major classes that catalyze phosphorylation of either serine and threonine, or tyrosine residues [2–4]. Their catalytic domains vary in length from 250 to 300 amino acids and contain conserved sequences responsible for ATP and peptide binding, and for phosphoryl transfer. Crystal structures of protein-serine/threonine and protein-tyrosine kinases solved in the presence of bound substrates have shown the requirement for a

specific conformation of ATP and bound bivalent cation(s) [2,3,5,6]. Many structures show at least one metal ion bound in the active site in the presence of ATP, whereas a second site is occupied in some cases. This metal ion is important to the catalytic mechanism of the enzyme, and all kinases contain a conserved motif, called ‘the DFG loop’, for the purpose of binding and positioning metal ions. The kinase domain of known eukaryotic protein kinases (ePKs) contains several conserved subdomains in addition to the DFG loop. The nucleotide-binding loop or ‘P-loop’, typically with the sequence GXGXXG, interacts with and orients the triphosphate moiety of the ATP. The catalytic

## Abbreviations

AfRio2, Rio2 from *Archaeoglobus fulgidus*; AMPPNP, 5'-adenylyl imidodiphosphate; ePK, eukaryotic protein kinase; PKA, cAMP-dependent protein kinase.

loop contains conserved Asn and Asp residues which are important for catalysis and metal binding and separated by three amino-acid residues. In addition to the loops that interact with the ATP molecule, canonical ePKs contain a loop known as the activation loop or subdomain VIII [1]. This subdomain is known to modulate the activity of some kinases through conformational changes on phosphorylation at a site within this loop. In addition, structural analysis of kinases bound to peptide substrates or substrate mimetics has shown that this loop plays a role in binding and recognition of the substrate. Subdomains IX and X of the catalytic domain of ePKs have also been shown to interact with peptide. These subdomains are highly conserved among ePKs that phosphorylate serine, threonine as well as tyrosine residues [1,4].

The RIO protein family is a group of serine protein kinases absolutely required for ribosome biogenesis in eukaryotes. They are classified as atypical protein kinases based on their lack of significant sequence homology to ePKs [7]. The RIO kinases can be divided into three subfamilies that share homology in the conserved RIO domain. Representatives of two of the subfamilies, Rio1 and Rio2, are universally present in organisms from archaea to man, suggesting a fundamental role in the cell [8,9]. Yeast Rio1 and Rio2 are essential gene products shown to have serine kinase activity *in vitro*; the presence of catalytically required residues is necessary for *in vivo* function [8–11]. A third subfamily, named Rio3, has been found thus far only in multicellular eukaryotes. Each subfamily contains distinct subfamily-specific conserved residues within the catalytic domain, and the Rio2 and Rio3 contain additional domains N-terminal to the RIO domain, unique in each subfamily.

Ribosomal RNA processing occurs in eukaryotic cells through a complex, stepwise process [12]. Studies in yeast have indicated that processing of 20S pre-rRNA to the 18S rRNA of the small ribosomal subunit absolutely requires both Rio1 and Rio2 [9,11,13]. Yeast Rio2 has also been found through tandem affinity purification studies to be associated with many factors involved in ribosome biogenesis and cell proliferation [13–15]. Reports have indicated that Rio2 enzymatic activity is necessary for cleavage of 20S pre-rRNA [8]. Rio2 proteins are functionally distinct from Rio1 proteins and do not complement their activity despite significant sequence similarity ( $\approx 43\%$  in yeast) [16]. However, the precise molecular function of Rio2, or the mechanism that distinguishes it from Rio1, is at present unknown.

Our previously solved crystal structures of Rio2 from *Archaeoglobus fulgidus*, a hyperthermophilic archaeal organism, have revealed the structure of the

RIO kinase domain and the winged-helix fold of the Rio2-specific N-terminal domain [17]. Despite the lack of significant sequence similarity to ePKs, the RIO kinase domain resembles a trimmed version of an ePK catalytic domain. The Rio2 catalytic domain contains all the structural features required for catalysis in ePKs but neither the activation (subdomain VII; APE) loop nor subdomains IX and X. Our previously reported structures from crystals soaked in ATP or 5'-adenylyl imidodiphosphate (AMPPNP) and  $MnCl_2$  showed the presence of a nucleotide bound in the nucleotide-binding pocket, but no metal ions [17]. As all kinases require one or more bivalent cations for catalysis, our interpretation was that these structures represented inactive forms of Rio2. We hypothesized that, within the constraints of the crystal lattice, Rio2 was unable to undergo the movement needed to bind ATP and  $Mn^{2+}$  ions in a catalytically relevant conformation. To test this hypothesis, we solved the structures of Rio2 from crystals grown in the presence of ATP or ADP and  $MnCl_2$ . In the structures presented here, two metal ions are found in the active site with bound ATP, and one metal ion is seen in the presence of ADP. Alignments with the previously solved structures of inactive Rio2 show significant movement within the kinase domain as well as ordering of several residues to accommodate and bind the  $\gamma$ -phosphate. We believe that these new structures represent the biologically relevant conformation of the Rio2 protein assumed upon ATP and ADP binding. We have also mapped the location of the autophosphorylation site in Rio2 to the disordered loop of the Rio2 kinase domain, where it might play a role in regulation of Rio2 kinase activity.

## Results

### Structure determination

Full-length Rio2 from *A. fulgidus* (AfRio2) was expressed in *Escherichia coli* and purified as described previously [17]. The enzyme was crystallized in the presence of  $MnCl_2$  and either ATP alone, or ADP and phosphoserine. Crystals of both the ATP and ADP complexes were isomorphous and belonged to the space group C2, with one molecule per asymmetric unit. Diffraction extending to resolution exceeding 1.85 Å could be measured on a synchrotron source. Both structures were solved by molecular replacement using the previously determined structure of apo-AfRio2. Data collection and crystallographic refinement statistics are summarized in Table 1.

Rio2 proteins contain two domains, the N-terminal Rio2-specific winged helix domain and the RIO kinase

**Table 1.** Data collection and refinement statistics for the ATP–Mn-bound and ADP–Mn-bound Rio2. Crystal data: space group C2.

	ATP–Mn <sup>2+</sup>	ADP–Mn <sup>2+</sup>
a (Å)	116.86	116.33
b (Å)	44.37	44.59
c (Å)	62.79	62.63
β (°)	94.01	93.88
Resolution (Å)	30–1.84	30–1.75
R <sub>sym</sub> (last shell)	0.035 (0.114)	0.035 (0.125)
Reflections	25770 (1333)	30487 (1622)
Redundancy	3.9 (3.8)	3.9 (3.7)
Completeness (%)	96.3 (68.2)	98.5 (87.3)
R/R <sub>free</sub> (%)	16.6/21.1	18.7/21.9
(Last shell)	(18.3/24.4)	(21.6/23.5)
Mean B factor (Å <sup>2</sup> )	21.5	24.8
Waters	355	290
RMS deviations		
Lengths (Å)	0.021	0.012
Angles (°)	1.83	1.32

domain (Fig. 1A). The RIO domain is structurally homologous to known protein kinase domains, which contain two lobes connected by a flexible linker. ATP and its analogs bind between the two lobes and, in most cases, the presence of a ligand results in a movement of one lobe relative to the other. This is seen in structures of Rio2 as well, and the largest movement of the N-lobe relative to the C-lobe is seen in the Rio2–ATP–Mn complex reported here (Fig. 1B). In the previously solved structures of Rio2, residues 125 through 141 (between β3 and αC) were disordered. In the structure of Rio2 bound to ATP and Mn, residues 125–127 are ordered and clearly seen in the electron density.

### Binding of ATP and ADP to Rio2

Our previous structures of Rio2 solved from crystals soaked in solutions containing Mn<sup>2+</sup> and ATP or

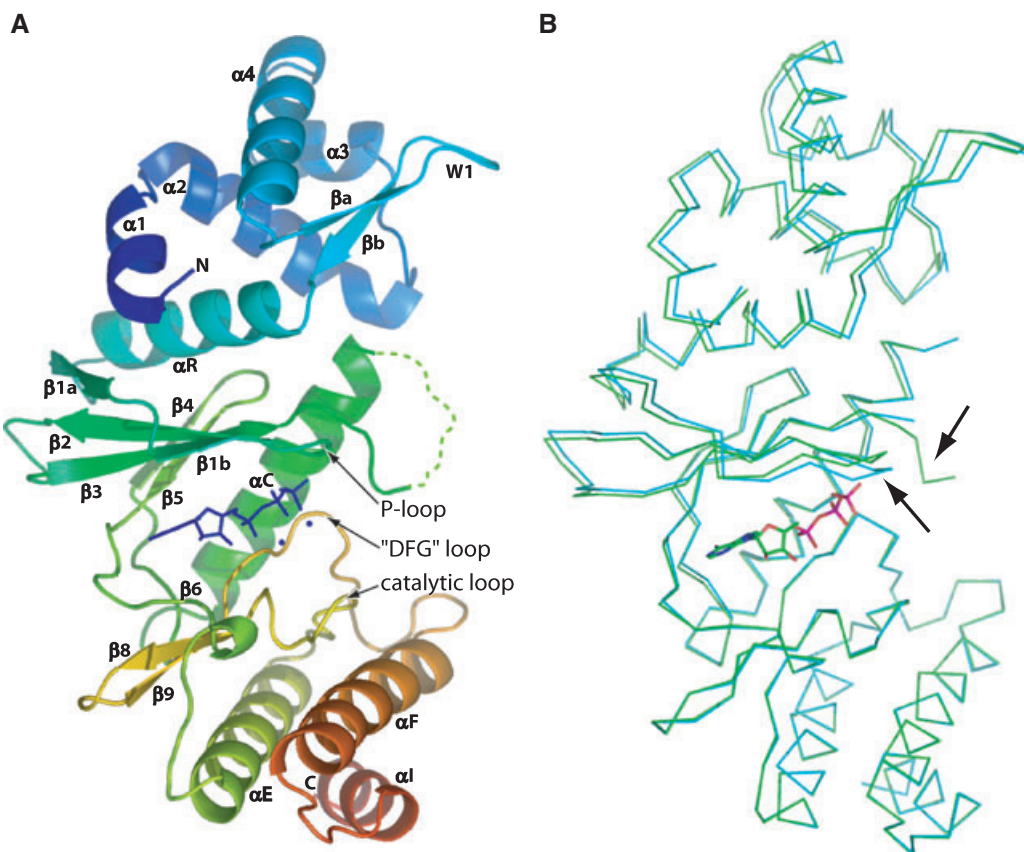


**Fig. 1.** Structure of Rio2 bound to ATP. (A) Structure of Rio2–ATP–Mn complex showing the winged helix domain (α1 to βb) and the RIO kinase domain (αR to αI) containing the N-lobe and C-lobe and the flexible disordered loop (dashed). The ATP molecule is shown in blue stick representation with the Mn<sup>2+</sup> ions drawn as small spheres. (B) Trace representation of Rio2 in the presence of ATP (green), aligned on apo-Rio2 using the C-lobe of the kinase domain, shows a slight movement of part of the N-lobe resulting in an opening of the active site compared with the apo structure (cyan; PDB code 1TQI). The arrows indicate movement of the nucleotide-binding loop and the ordered portion of the flexible loop.

AMPPNP showed no metal binding in the active site, and no direct contacts between the  $\gamma$ -phosphate and protein residues. Thus, we hypothesized that the conformation observed in these structures represented an inactive form of Rio2. In the structures presented here, bound  $Mn^{2+}$  is clearly seen in the active site (Fig. 2). In the ATP structure, two metal ions (Mn1 and Mn2) are clearly visible, whereas in the ADP structure only one metal ion (Mn1) can be seen (Fig. 2). As shown in Fig. 2, the two metal ions in the ATP structure are coordinated by one phosphate oxygen from each of the three phosphate groups of ATP, by two of the conserved catalytic residues (Asn223 and Asp235), by an RIO domain-specific conserved Glu103, as well as by an ordered phosphate from the crystallization buffer. Water molecules complete the coordination spheres of both metal ions. The  $\gamma$ -phosphate is held in place through coordination with one of the metal ions (Mn2, bond length 2.14 Å) and interactions with His122, His126, and Lys120 (bond lengths 3.09, 2.62, and 2.72 Å, respectively). The latter residue is the conserved

lysine present in all protein kinases, His122 is highly conserved in Rio2 proteins, and His126 is replaced by an arginine in most Rio2 proteins other than AfRio2. This substitution correlates with the identity of the preceding residue, which is a valine in AfRio2 but a leucine in all Rio2 proteins that contain Arg at the His126 position.

Lys120 also forms a 2.68-Å hydrogen bond with the  $\alpha$ -phosphate of ATP, in addition to its interaction with the  $\gamma$ -phosphate. The  $\alpha$ -phosphate position is also coordinated via a 2.27 Å bond to Mn1. Ser104, conserved in Rio2 proteins and located in the nucleotide-binding loop, forms a 2.69 Å hydrogen bond with the  $\beta$ -phosphate, contributing to the opening of the active site relative to the apo structure. The  $\beta$ -phosphate is also held firmly in place through coordination with both Mn1 and Mn2 (bond lengths 2.32 and 2.33 Å, respectively). The ordered phosphate ion from the buffer is hydrogen-bonded to the catalytic Asp218 (2.44 Å) and is within 2.32 Å of both metal ions.

Rio2 binds ATP in a different conformation from typical serine/threonine or tyrosine kinases such as

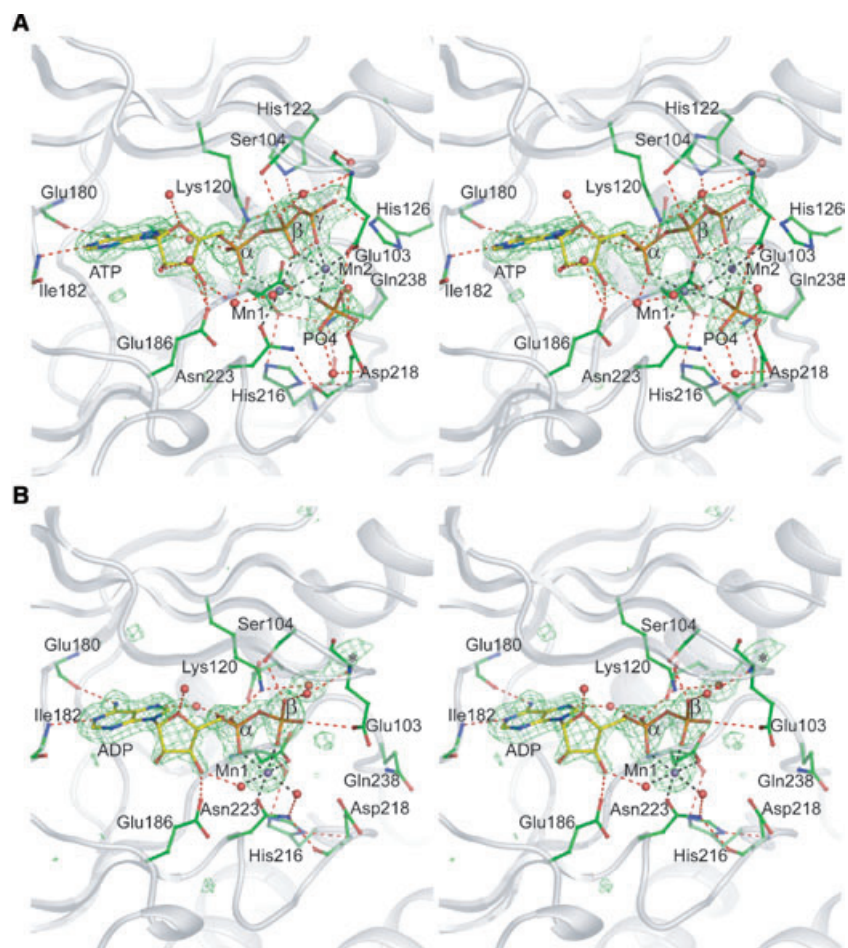


**Fig. 2.** Active site of Rio2 with ATP and ADP and metal ions. (A) Omit map of the interior cavity of the active site of Rio2 contoured at  $3\sigma$ . The  $F_o - F_c$  map was calculated using a refined model that contained no nucleotide or metal ions, with data collected from the Rio2–ATP–Mn cocrystal. Hydrogen bonds are shown as dashed red lines (distance  $< 3.2$  Å). Coordinate bonds are shown as dashed black lines. (B) An analogous representation for the Rio2–ADP–Mn dataset. The coordinates of the nucleotides resulting from the final refinements are superimposed on the maps in (A) and (B). Water molecules are represented by red spheres, and density attributed to weak phosphoserine binding is indicated by an asterisk in (B).

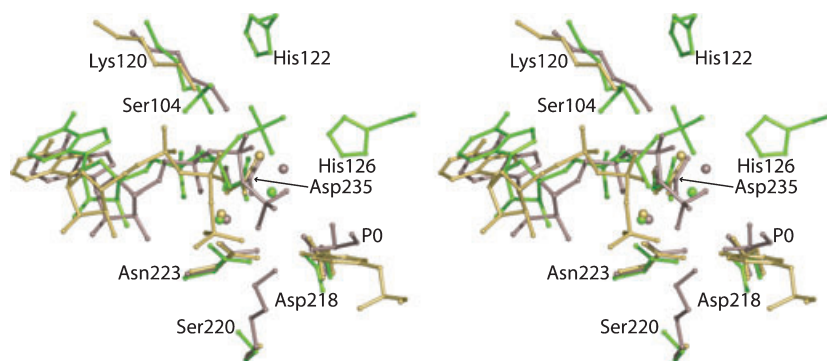


**Fig. 3.** ATP conformation is unique in Rio2. Alignment of the catalytic loop and the metal-binding loop of Rio2 (green) with that of PKA (pink; PDB code 1ATP) and insulin receptor tyrosine kinase (yellow; PDB code 1IR3) shows the difference in the  $\gamma$ -phosphate conformation of ATP bound to Rio2. The catalytic and metal-binding residues, as well as residues that interact with the  $\gamma$ -phosphate are shown and labeled with Rio2 numbering. The spheres show the positions of the metal ions. The residues that indicate the positions of the phosphorylated residues for the PKA and insulin receptor tyrosine kinase peptide substrates are labeled P0.

cAMP-dependent protein kinase (PKA) and insulin receptor tyrosine kinase (Fig. 3) [18,19]. In particular, the position of the  $\gamma$ -phosphate is significantly shifted relative to the position of the metal ions and the catalytic residues. This is highlighted by the absence in Rio2 of the equivalent of PKA Lys168, which contacts one of the phosphate oxygens of the  $\gamma$ -phosphate in these kinases [18]. This lysine is conserved in most serine/threonine ePKs, but not in the tyrosine kinases [1]. In AfRio2, this residue is replaced by Ser220, and is either Ser or Asp in other Rio2 proteins. Ser220 contacts the backbone amide of conserved Tyr222. As Tyr222 is not involved in the stabilization of the 3D structure of the kinase domain, we believe that this residue is conserved for the purpose of providing substrate recognition. Therefore, Ser220 may be important for keeping this residue in a functional conformation. Another factor that influences the positioning of the  $\gamma$ -phosphate is the interaction of conserved Ser104 with one of the phosphate oxygens of the  $\beta$ -phosphate. This interaction would prevent the positioning of the phosphates in the Rio2 protein in the conformation observed in the other kinases. Several direct contacts are made with the  $\gamma$ -phosphate by residues in Rio2 to hold it firmly in that position (Fig. 2).

### Conformation changes upon the binding of ATP by Rio2

Comparison of the previously determined structure of the presumably nonfunctional Rio2–AMPPNP complex and the structure of Rio2–ATP–Mn complex presented here indicated a range of conformational changes required for productive nucleotide binding. Although the adenosine ring of AMPPNP was able to

bind in the ATP-binding pocket of Rio2 when the nucleotide was soaked into the crystals, binding of the  $\gamma$ -phosphate and metal ions required repositioning of several residues and led to movement of the nucleotide-binding loop (Fig. 3). The  $\gamma$ -phosphate binds in a pocket that is not present in the AMPPNP structure, suggesting that a conformational movement is required to allow the phosphate to create and enter the pocket. The  $\gamma$ -phosphate is sealed in the pocket by interactions with Glu103 and with two histidine residues. One of them, His126, belongs to the previously described disordered loop of the enzyme, indicating that this part of the structure becomes ordered as a consequence of proper ATP binding. The catalytically important Asn223 changes conformation in order to bind the metal ion, and Lys120 moves to contact phosphate oxygens from both the  $\alpha$ -phosphate and  $\gamma$ -phosphate. The resulting overall movement of the N-lobe of Rio2 relative to the C-lobe creates a more open active site. This opening of the active site is in sharp contrast with many reported structures of protein kinase–ATP complexes. In general, such structures show a closing of the active site upon binding to ATP. This difference may be a direct result of the altered binding conformation of ATP in the Rio2 active site compared with ePKs. The binding of the  $\gamma$ -phosphate much deeper underneath the nucleotide-binding loop results in shifting of the loop further away from the center of the active site.

### Comparison of the ATP–Rio2 and ADP–Rio2 reveals gated binding of the $\gamma$ -phosphate

The crystals used to solve the structure of Rio2 in complex with ADP and  $Mn^{2+}$  were obtained from cocrystallization of Rio2 with ADP,  $MnCl_2$ , and phos-

phoserine. The weak electron density observed for the phosphoserine was insufficient for detailed modeling of this component. Strong electron density was seen for ADP and one of the  $Mn^{2+}$  cations (Fig. 2). Therefore, one metal-binding site appears to be occupied only in the presence of the  $\gamma$ -phosphate. Although the structures of the enzyme in the presence of ATP and ADP are very similar, with almost no movement of the N-lobe and C-lobe relative to each other, specific residue movements are observed. In particular, His126 and Thr127, ordered in the presence of ATP, are disordered in the presence of ADP (Fig. 4A). A weak density that we interpreted as belonging to phosphoserine suggests a position for the P<sub>0</sub> site near the vacated position of these two residues (Fig. 2B). This means that, upon substrate binding, these residues may need to move out of the way, acting like a ‘gate’, to allow the approach of the substrate serine to the  $\gamma$ -phosphate of ATP. This is also observed in comparing the Rio2–ATP–Mn complex with the previous structure of Rio2 soaked in AMPPNP (Fig. 4B). Analysis of a surface representation of the active site with bound ATP or ADP shows that the  $\gamma$ -phosphate is completely buried in the presence of ATP but not ADP, indicating a requirement for such an opening to occur before catalysis can take place (Fig. 4C,D). In addition, movement of conserved Gln238 is observed in a comparison of the two structures (Fig. 2). In the ATP–Mn complex, the side chain amino group of Gln238 forms hydrogen bonds to the backbone carbonyl oxygen of

catalytic loop and metal-binding loop residues His216 and Asp235 (Fig. 2A). In the presence of ADP, Gln238 is rotated away from the active site and does not interact with it (Fig. 2B). This relocation may be a direct consequence of the movement of His126, which packs against the aliphatic portion of Gln238 when ATP is bound. Therefore, the movement of this portion of the flexible loop may not only stabilize  $\gamma$ -phosphate binding, but also result in the stabilization of the metal-binding and catalytic loops through the interactions with Gln238.

### Rio2 autophosphorylates a conserved serine of the disordered loop

We have previously shown that the Rio2 protein becomes autophosphorylated during incubation of the enzyme with [<sup>32</sup>P]ATP[ $\gamma$ P], although the site of phosphorylation was not established [17]. Radiolabeled Rio2 enzyme was now subjected to phosphopeptide mapping and sequencing to determine the site at which autophosphorylation occurs (Fig. 5). Phosphoamino-acid analysis of radiolabeled Rio2 showed that only serine residues were phosphorylated (Fig. 5A). Only a single radioactive peptide peak was obtained after HPLC separation of peptides obtained from complete digestion with Lys-C, an enzyme that cleaves peptide bonds C-terminal to lysine residues (Fig. 5B). This result suggests that autophosphorylation of Rio2 is limited to a single site. Phosphopeptide sequencing of

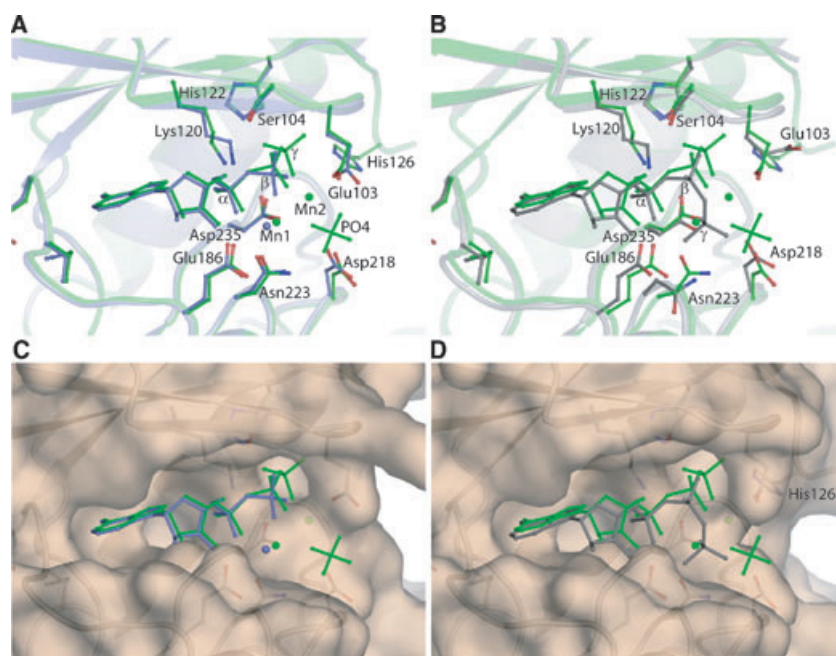


**Fig. 4.** Conformational changes in Rio2 upon ATP binding. (A) Alignment of the ATP-bound (blue) and ADP-bound (green) Rio2 structures showing the active-site loops and the nucleotides. (B) Alignment of the ATP-bound Rio2 structure with the previously reported AMPPNP (gray) complex (PDB code 1TQM). (C) A surface view of the active site bound to ADP (blue) with ATP (green) aligned. (D) A surface view of the active site bound to ATP (green) showing the aligned AMPPNP molecule.

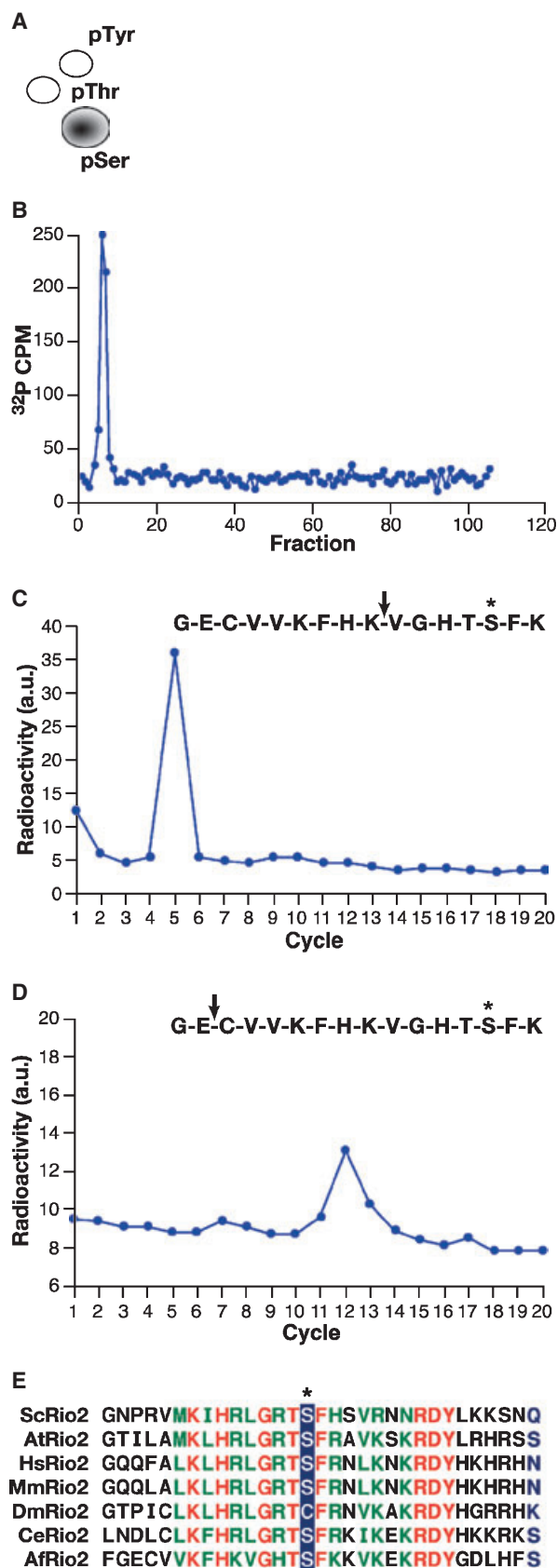


**Fig. 5.** Autophosphorylation of Rio2 on Ser128. (A) Phosphoamino-acid analysis of phosphorylated Rio2. The positions of the ninhydrin-stained standards are indicated on the autoradiogram of the AfRio2 sample by open circles, labeled for each phosphoamino acid. (B) Radioactivity levels of HPLC fractions after cleavage with Lys-C protease. (C) Phosphopeptide sequencing of the labeled Lys-C peptide of Rio2. The Lys-C cleavage site is indicated by an arrow in the inset sequence corresponding to residues 215–244 of AfRio2. The residue eluted after the 5th cycle is indicated by an asterisk. (D) Phosphopeptide sequencing of the labeled Glu-C peptide of Rio2. The Glu-C cleavage site is indicated as in (C). The residue eluted after the 12th cycle is indicated by an asterisk. (E) Conservation of the autophosphorylation site of Rio2. The phosphorylated serine is highlighted by the blue box.

peptides resulting from Lys-C digestion, as well as from proteolysis by Glu-C, an enzyme that cleaves C-terminal to glutamic acid residues, indicated that the radiolabeled amino acid was released after the 5th and 12th cycle, respectively (Fig. 5C,D). Analysis of the sequence of AfRio2 indicated that autophosphorylation at Ser128 is the only possibility consistent with these data. As shown in Fig. 1, a segment consisting of 18 amino acids (residues 127 through 143), presumably forming a large loop, is disordered in the Rio2–ATP complex. In the absence of the  $\gamma$ -phosphate, two more residues, 126 and 127, become disordered, thus Ser128 is not directly observed in any of the structures. However, this residue is directly adjacent to the part of the loop that changes conformation in response to ATP binding. Analysis of the conservation of this residue among Rio2 homologs shows that not only Ser128, but also the surrounding residues are highly conserved, and, among the eukaryotic homologs, the only variation is a cysteine in the *Drosophila melanogaster* Rio2 (Fig. 5E).

## Discussion

The structures of Rio2 with bound Mn–ATP and Mn–ADP presented here indicate that significant changes must occur in Rio2 proteins in order for them to bind a nucleotide in a productive fashion. The large extent of these movements prevented their occurrence within the confines of the crystal. Therefore, when the nucleotide was soaked in, it bound in the active site in a non-physiological manner that precluded binding of the metal ions. However, when binding of the ATP took place in solution, the process was accompanied by creation of metal-binding sites. In other words, the binding of metal ions appears to be secondary to the correct positioning of the phosphates in the active site. When these groups are incorrectly positioned, as in the case of the AMPPNP complex obtained by soaking of

pregrown crystals, binding of the metal ions does not occur. The structure of the Mn–ATP complex also reiterates the requirement of metal ions for the correct positioning of residues important for catalysis.

The mode of binding of ATP in the active site of Rio2 is unusual among protein kinases. The  $\gamma$ -phosphate of the ATP is in a different position in Rio2 from in serine/threonine and tyrosine ePKs. In serine ePKs, the  $\gamma$ -phosphate is exposed and accessible. In Rio2, the interaction of the  $\gamma$ -phosphate with His126 and the interaction of the second metal ion with Glu103 results in a conformation in which there is no direct access to the  $\gamma$ -phosphate. Therefore, we believe that in order for phosphotransfer to take place, the loop that includes His126 must move to allow access of the serine (which will occupy the P0 substrate-binding site) to the active site. Although in the absence of a productive complex with a substrate or substrate analog we are still unable to create a detailed model of the binding of a substrate peptide to the enzyme, we believe that a site for the modified serine is created through movement of the loop containing His126, Thr127, and Ser128. This assumption is supported by the fact that this region is very dynamic, as shown by its disorder when no  $\gamma$ -phosphate is present (in apo and ADP structures). The probable P0 position which is marked in Fig. 6 is based on the weak electron density observed in the Rio2–ADP–Mn structure, which we attribute to the binding of phosphoserine. This density was insufficient to model the complete modified amino acid, but significantly too large to be accounted for by water molecules.

The positioning of the  $\gamma$ -phosphate in Rio2 places the proposed kinase catalytic base, Asp218, too far away to be able to participate directly in phosphorylation. Whereas the distance between the carboxyl oxygen of the Asp and the phosphorus atom is  $\approx 3.6$  Å in PKA, this distance is nearly 5.8 Å in Rio2. This raises the possibility that the conformation of the nucleotide seen in the structure of the ATP–Rio2 complex may still not correspond to the final, productive one. However, the presence of three interactions through the phosphate oxygens with conserved residues argues strongly that the observed position of the  $\gamma$ -phosphate should indeed be functional. In addition, our recently determined structure of the AfRio1–ATP–Mn complex (unpublished) shows that the  $\gamma$ -phosphate adopts a similar orientation, lending support to the idea that this might be an RIO kinase-specific feature. If indeed the  $\gamma$ -phosphate is positioned ready for catalysis, the altered positioning would support our previously advanced hypothesis that Rio2 binds its substrate in a distinct manner compared with ePKs,

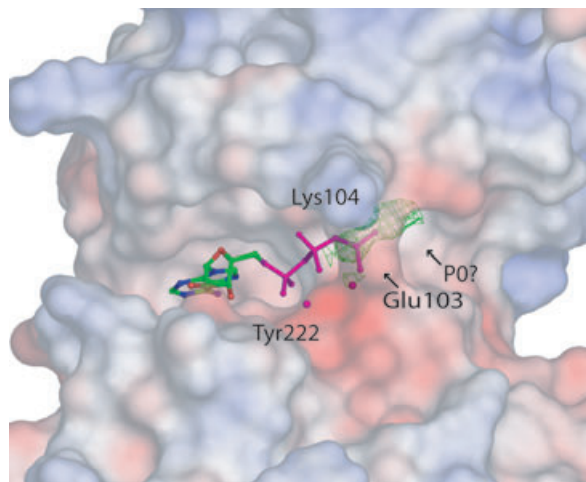


**Fig. 6.** Possible P0 position of Rio2 peptide substrate. A transparent electrostatic surface representation of the Rio2 active site from the Rio2–ADP–Mn complex is shown, with the ATP molecule from the Rio2–ATP–Mn complex modeled in through alignment of the two structures (red is negative, blue is positive). The green mesh (mostly occluded in a cavity underneath Glu103) is the remaining positive density observed in the Rio2–ADP–Mn active site, contoured at  $3\sigma$ . The arrow indicates the suggested position of the serine that is being phosphorylated.

based on the seeming lack of known substrate-binding loops in Rio2. However, this would not explain the role of Asp218 in catalysis in the Rio2 proteins. It has been shown that mutation of this residue produces a largely inactive yeast Rio1 enzyme, but a partially active yeast Rio2 [8]. Our unpublished data for *A. fulgidus* Rio1 also show a significant decrease in autophosphorylation activity when the catalytic Asp is mutated to Ala.

The site at which autophosphorylation occurs is highly conserved, as are the residues surrounding it. This degree of conservation suggests that Rio2 proteins specifically autophosphorylate at this sequence and that specific residues in the kinase domain recognize the phosphorylation site. Therefore, despite the lack of subdomains responsible for substrate interactions in ePKs, specific substrate recognition probably does occur in RIO proteins. Our previous analysis of the conserved surface residues of Rio2 indicated a large, conserved surface surrounding its active site. This led to the postulate that Rio2 may recognize a protein surface, rather than just a peptide. Although this may still hold, the presence of the modified serine in a flexible loop allows the possibility that Rio2 may recognize an extended peptide. Studies are presently under way to determine the structural elements necessary for Rio2–peptide substrate interactions.

The autophosphorylation of a serine residue so close to the segment of the molecule that interacts with the  $\gamma$ -phosphate suggests a regulatory role for this phosphorylation site. Phosphorylation at this site could change the manner in which this part of the loop responds to ATP binding and thus regulate the activity of the molecule. More studies are required to test the importance of this site to the function of Rio2. If it is indeed the case that this serine is important for the regulation of the enzymatic activity, this may indicate that the activation or ‘APE’ loops of canonical serine kinases are substituted by the flexible loop seen in the RIO kinases.

## Experimental procedures

### Crystallization of Rio2–ATP–Mn and Rio2–ADP–Mn

The full-length recombinant Rio2 was prepared for crystallization as previously described [17]. In order to cocrystallize Rio2 with nucleotide substrates, the protein solution was diluted twofold with crystallization buffer including 40 mM ATP or ADP and 40 mM  $\text{MnCl}_2$ . In the case of the ADP complex, 40 mM phosphoserine was also present. The protein was subsequently concentrated to the original volume, resulting in the final 20 mM concentration of ATP, ADP, phosphoserine, and  $\text{MnCl}_2$ . The crystals were grown by hanging drop vapor diffusion in 1-mL wells containing 5–12% poly(ethylene glycol) 900 and 100 mM sodium phosphate/citrate buffer, pH 3.6–4.1. Crystals grew large enough for X-ray diffraction studies after 4–5 days at 20 °C.

### Data collection and processing

Crystals were flash frozen in mother liquor containing 20% ethylene glycol. Diffraction data were collected at 100 K with a MAR300 CCD detector at the SER-CAT beamline 22-ID, located at the Advanced Photon Source, Argonne National Laboratory (Argonne, IL, USA). All data were integrated and merged using HKL2000 [20]. Table 1 contains details on data statistics for all data sets.

### Structure determination and refinement

The structures were solved by molecular replacement using as a search model the previously described structure of Rio2, utilizing the program MOLREP within the CCP4 program suite [21]. ARP/WARP [22] was used to perform automatic model building using the phases obtained from molecular replacement. The ligands were placed in the models and the structures were finalized by rebuilding in XTALVIEW [23] and refinement with REFMAC5 [24].  $R_{\text{free}}$  was monitored by using 5% of the reflections as a test set for

each structure. The refinement statistics are provided in Table 1. The final coordinates and structure factors have been submitted to the Protein Data Bank (accession codes 1ZAO for the AfRio2–ATP–Mn and 1ZAR for AfRio2–ADP–Mn). The figures that depict the structures of Rio2 were created using PYMOL [25]. In Fig. 6, the program APBS (adaptive Poisson–Boltzmann solver) was used as a PYMOL plug-in to generate and display the electrostatic surface [26].

### Radiolabeling of AfRio2

To produce radiolabeled AfRio2 in order to determine its autophosphorylation site(s), the enzyme was incubated for 90 min at 40 °C in the presence of  $^{32}\text{P}$ -labeled ATP. The reaction buffer contained 50 mM NaCl, 50 mM Tris/HCl, pH 7.5, and 20  $\mu\text{Ci}$  [ $^{32}\text{P}$ ]ATP[ $\gamma\text{P}$ ] with 2 mM  $\text{MgCl}_2$ . All reactions contained 60  $\mu\text{g}$  of the enzyme. Half of the reaction mixtures were run in each lane (30  $\mu\text{g}$  protein) of a NuPAGE 4–12% Bis-Tris denaturing gel (Invitrogen, Carlsbad, CA, USA) for 1 h at 120 V. The labeled protein was then transferred on to Invitrolon P (Invitrogen) membrane using Xcell Blot II apparatus (Invitrogen) as per the manufacturer’s instructions. The resulting membrane was used to expose a film for 30 min to determine the position of the labeled bands, and the bands were cut out for phosphoamino-acid analysis and phosphopeptide mapping and sequencing.

### Phosphoamino-acid analysis

A portion of the membrane was hydrolyzed in 200  $\mu\text{L}$  4 M HCl at 110 °C for 1.5 h. Phosphoamino-acid standards were added and the solution was lyophilized. The contents were redissolved in electrophoresis buffer (acetic acid/formic acid/water, 15 : 5 : 80, v/v/v) and applied to 20  $\times$  20 cm cellulose TLC plates. The plate was electrophoresed at 1500 V for 40 min then rotated 90 ° and subjected to chromatography overnight using 0.5 M  $\text{NH}_4\text{OH}$ /isobutyric acid (30 : 50, v/v). The plate was dried and sprayed with ninhydrin to localize the phosphoamino-acid standards. Radioactivity was detected and visualized with a Typhoon model 9200 phosphoimager (Amersham Biosciences, Little Chalfont, Bucks, UK).

### Phosphopeptide mapping

The membrane was cut into small pieces and washed sequentially with methanol, distilled water, and then blocked with 1.5% PVP-40 in 100 mM acetic acid. Membranes were digested with either Glu-C or Lys-C proteases (Roche, Indianapolis, IN, USA) in 50 mM  $\text{NH}_4\text{HCO}_3$ , pH 8, overnight. Supernatants containing released peptides were removed, adjusted to pH 2 with 20% (v/v) aqueous

trifluoroacetic acid and subjected to RP-HPLC on a Waters (Milford, MA, USA) C<sub>18</sub> column (3.9 × 300 mm). The column was developed with a gradient of 0–30% (v/v) acetonitrile in 0.05% (v/v) aqueous trifluoroacetic acid over 90 min at a flow rate of 1 mL·min<sup>-1</sup>. Fractions of volume 1 mL were collected and counted for <sup>32</sup>P in a Beckman (Fullerton, CA, USA) 6500 liquid-scintillation counter [27]. <sup>32</sup>P-labeled peptides were coupled to Sequelon disks and subjected to solid-phase Edman degradation with a model 492 Applied Biosystems (Foster City, CA, USA) peptide sequencer. Cycle fractions were collected on to Whatman (Florham Park, NJ, USA) #1 paper discs, and radioactivity was quantitated using a Typhoon (Amersham Biosciences, Little Chalfont, Bucks, UK) phosphoimager.

## Acknowledgements

We are grateful to Sook M. Lee and Peter F. Johnson, NCI-Frederick, for assistance with radioactive labeling of Rio2. Diffraction data were collected at the Southeast Regional Collaborative Access Team (SER-CAT) beamline 22-ID, located at the Advanced Photon Source, Argonne National Laboratory, Argonne, IL, USA. Use of the Advanced Photon Source was supported by the US Department of Energy, Office of Science, Office of Basic Energy Sciences, under Contract No. W-31-109-Eng38.

## References

- 1 Hanks SK & Hunter T (1995) Protein kinases 6. The eukaryotic protein kinase superfamily: kinase (catalytic) domain structure and classification. *FASEB J* **9**, 576–596.
- 2 Bossemeyer D (1995) Protein kinases: structure and function. *FEBS Lett* **369**, 57–61.
- 3 Engh RA & Bossemeyer D (2002) Structural aspects of protein kinase control: role of conformational flexibility. *Pharmacol Ther* **93**, 99–111.
- 4 Hanks SK, Quinn AM & Hunter T (1988) The protein kinase family: conserved features and deduced phylogeny of the catalytic domains. *Science* **241**, 42–52.
- 5 Knighton DR, Zheng JH, Ten Eyck LF, Ashford VA, Xuong NH, Taylor SS & Sowadski JM (1991) Crystal structure of the catalytic subunit of cyclic adenosine monophosphate-dependent protein kinase. *Science* **253**, 407–414.
- 6 Knighton DR, Zheng JH, Ten Eyck LF, Xuong NH, Taylor SS & Sowadski JM (1991) Structure of a peptide inhibitor bound to the catalytic subunit of cyclic adenosine monophosphate-dependent protein kinase. *Science* **253**, 414–420.
- 7 Manning G, Whyte DB, Martinez R, Hunter T & Sudarsanam S (2002) The protein kinase complement of the human genome. *Science* **298**, 1912–1934.
- 8 Geerlings TH, Faber AW, Bister MD, Vos JC & Raue HA (2003) Rio2p, an evolutionarily conserved, low abundant protein kinase essential for processing of 20S pre-rRNA in *Saccharomyces cerevisiae*. *J Biol Chem* **278**, 22537–22545.
- 9 Vanrobays E, Gelugne JP, Gleizes PE & Caizergues-Ferrer M (2003) Late cytoplasmic maturation of the small ribosomal subunit requires RIO proteins in *Saccharomyces cerevisiae*. *Mol Cell Biol* **23**, 2083–2095.
- 10 Angermayr M & Bandlow W (2002) RIO1, an extraordinary novel protein kinase. *FEBS Lett* **524**, 31–36.
- 11 Vanrobays E, Gleizes PE, Bousquet-Antonelli C, Noaillac-Depeyre J, Caizergues-Ferrer M & Gelugne JP (2001) Processing of 20S pre-rRNA to 18S ribosomal RNA in yeast requires Rrp10p, an essential non-ribosomal cytoplasmic protein. *EMBO J* **20**, 4204–4213.
- 12 Granneman S & Baserga SJ (2004) Ribosome biogenesis: of knobs and RNA processing. *Exp Cell Res* **296**, 43–50.
- 13 Schafer T, Strauss D, Petfalski E, Tollervey D & Hurt E (2003) The path from nucleolar 90S to cytoplasmic 40S pre-ribosomes. *EMBO J* **22**, 1370–1380.
- 14 Gavin AC, Bosche M, Krause R, Grandi P, Marzioch M, Bauer A, Schultz J, Rick JM, Michon AM, Cruciat CM *et al.* (2002) Functional organization of the yeast proteome by systematic analysis of protein complexes. *Nature* **415**, 141–147.
- 15 Ho Y, Gruhler A, Heilbut A, Bader GD, Moore L, Adams SL, Millar A, Taylor P, Bennett K, Boutilier K *et al.* (2002) Systematic identification of protein complexes in *Saccharomyces cerevisiae* by mass spectrometry. *Nature* **415**, 180–183.
- 16 Giaever G, Chu AM, Ni L, Connelly C, Riles L, Veronneau S, Dow S, Lucau-Danila A, Anderson K, Andre B *et al.* (2002) Functional profiling of the *Saccharomyces cerevisiae* genome. *Nature* **418**, 387–391.
- 17 LaRonde-LeBlanc N & Wlodawer A (2004) Crystal structure of *A. fulgidus* Rio2 defines a new family of serine protein kinases. *Structure (Camb)* **12**, 1585–1594.
- 18 Zheng J, Knighton DR, Ten Eyck LF, Karlsson R, Xuong N, Taylor SS & Sowadski JM (1993) Crystal structure of the catalytic subunit of cAMP-dependent protein kinase complexed with MgATP and peptide inhibitor. *Biochemistry* **32**, 2154–2161.
- 19 Hubbard SR (1997) Crystal structure of the activated insulin receptor tyrosine kinase in complex with peptide substrate and ATP analog. *EMBO J* **16**, 5572–5581.
- 20 Otwinowski Z & Minor W (1997) Processing of X-ray diffraction data collected in oscillation mode. *Methods Enzymol* **276**, 307–326.
- 21 CCP4 (1994) Collaborative Computational Project, Number 4, 1994. The CCP4 Suite: Programs for Protein Crystallography. *Acta Crystallogr* **D50**, 760–763.

- 22 Perrakis A, Morris R & Lamzin VS (1999) Automated protein model building combined with iterative structure refinement. *Nat Struct Biol* **6**, 458–463.
- 23 McRee DE (1999) XtalView/Xfit: a versatile program for manipulating atomic coordinates and electron density. *J Struct Biol* **125**, 156–165.
- 24 Murshudov GN, Vagin AA & Dodson EJ (1997) Refinement of macromolecular structures by the maximum-likelihood method. *Acta Crystallogr* **D53**, 240–255.
- 25 DeLano WL (2002) *The PyMOL Molecular Graphics System*. DeLano Scientific, San Carlos, CA.
- 26 Baker NA, Sept D, Joseph S, Holst MJ & McCammon JA (2001) Electrostatics of nanosystems: application to microtubules and the ribosome. *Proc Natl Acad Sci USA* **98**, 10037–10041.
- 27 Morrison DK, Heidecker G, Rapp UR & Copeland TD (1993) Identification of the major phosphorylation sites of the Raf-1 kinase. *J Biol Chem* **268**, 17309–17316.